Supporting Information for:

A Modular Advanced Oxidation Process Enabled by Cathodic Hydrogen Peroxide Production

James M. Barazesh,[#] Tom Hennebel,[#] Justin T. Jasper and David L. Sedlak[*]

Department of Civil and Environmental Engineering, 407 O'Brien Hall, University of California, Berkeley, CA 94720-1716, USA

# - These authors contributed equally

19 pages
7 tables
12 figures

*Corresponding author: sedlak@berkeley.edu, T: 510-643-0256, F: 202-354-4914

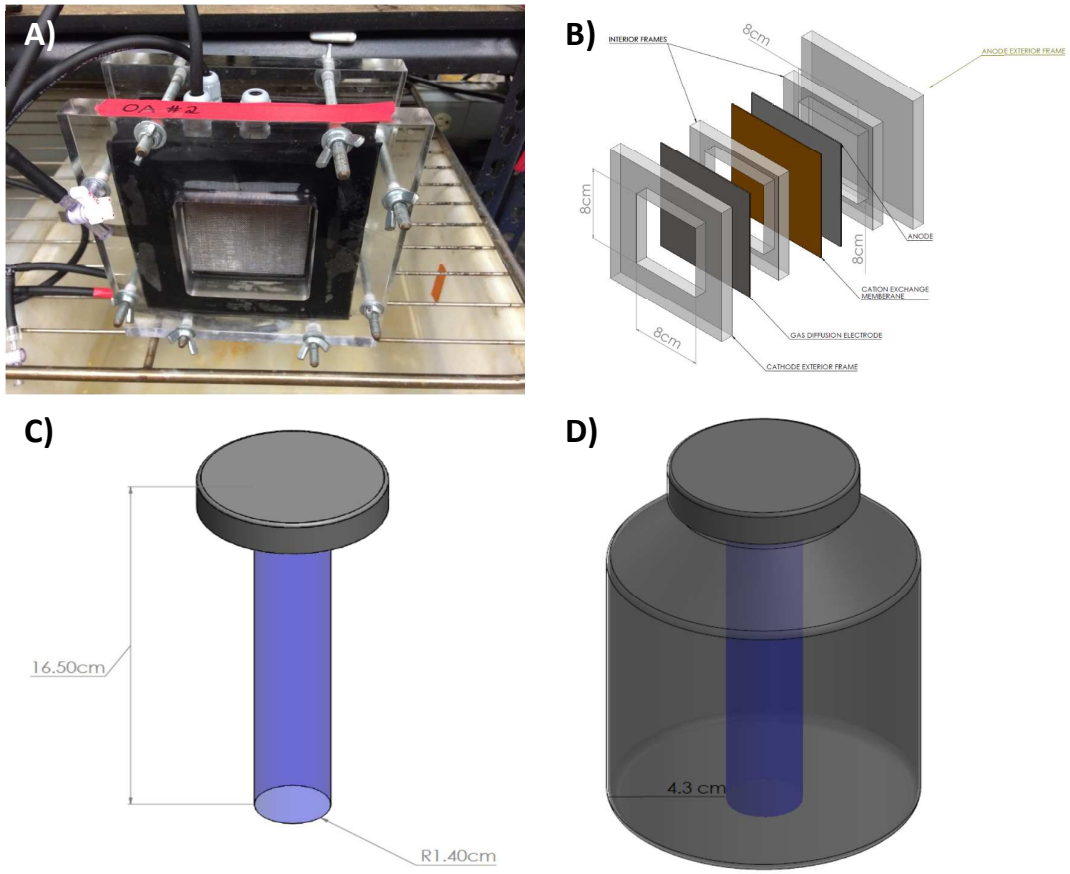

Figure S1: (a) Photo of the electrochemical cell, (b) blown up schematic of the cell components, (c) Low pressure UV lamp (G23 Odyssea Pool Lamp, 9W, electrical efficiency = 27%), (d) UV reactor.

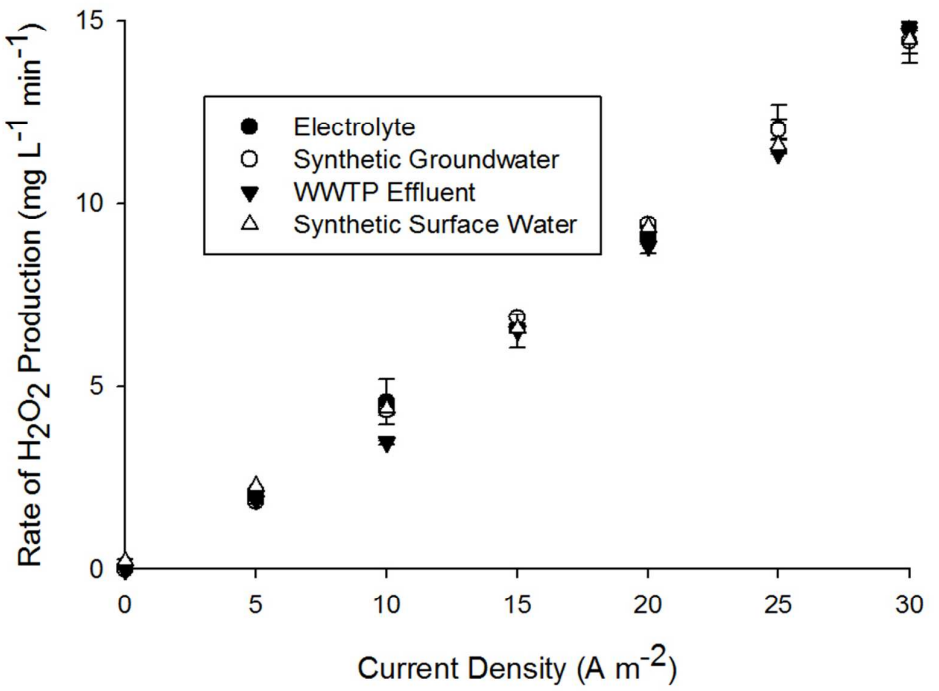

Figure S2: Hydrogen peroxide production rate as a function of current density (WWTP: wastewater treatment plant).

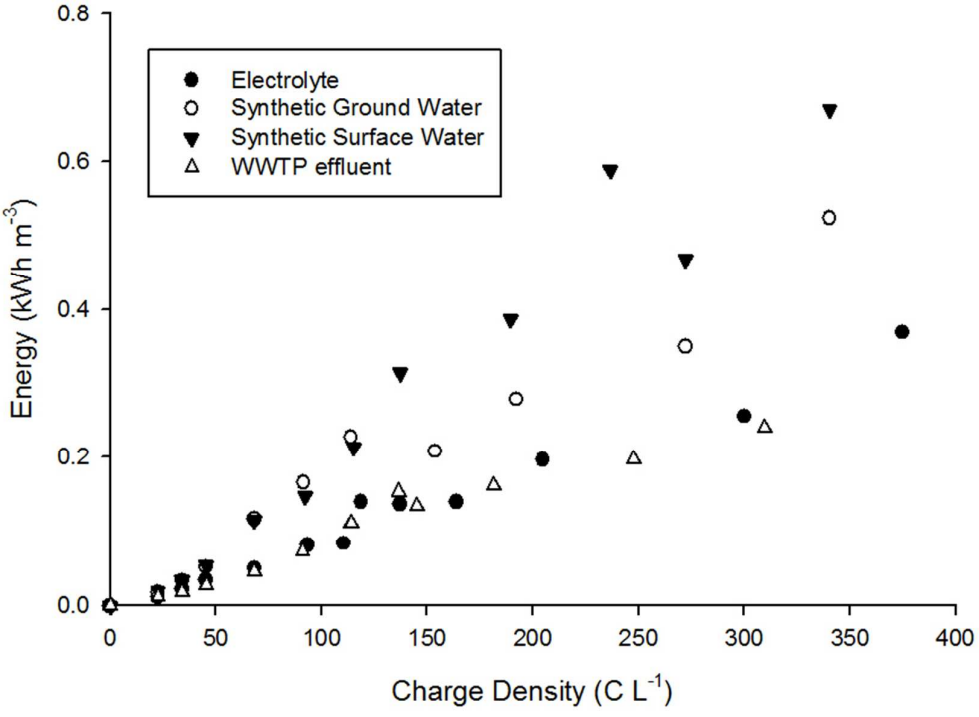

Figure S3: Energy demand of the electrochemical cell per m^3 of treated water as a function of applied charge density (WWTP: wastewater treatment plant).

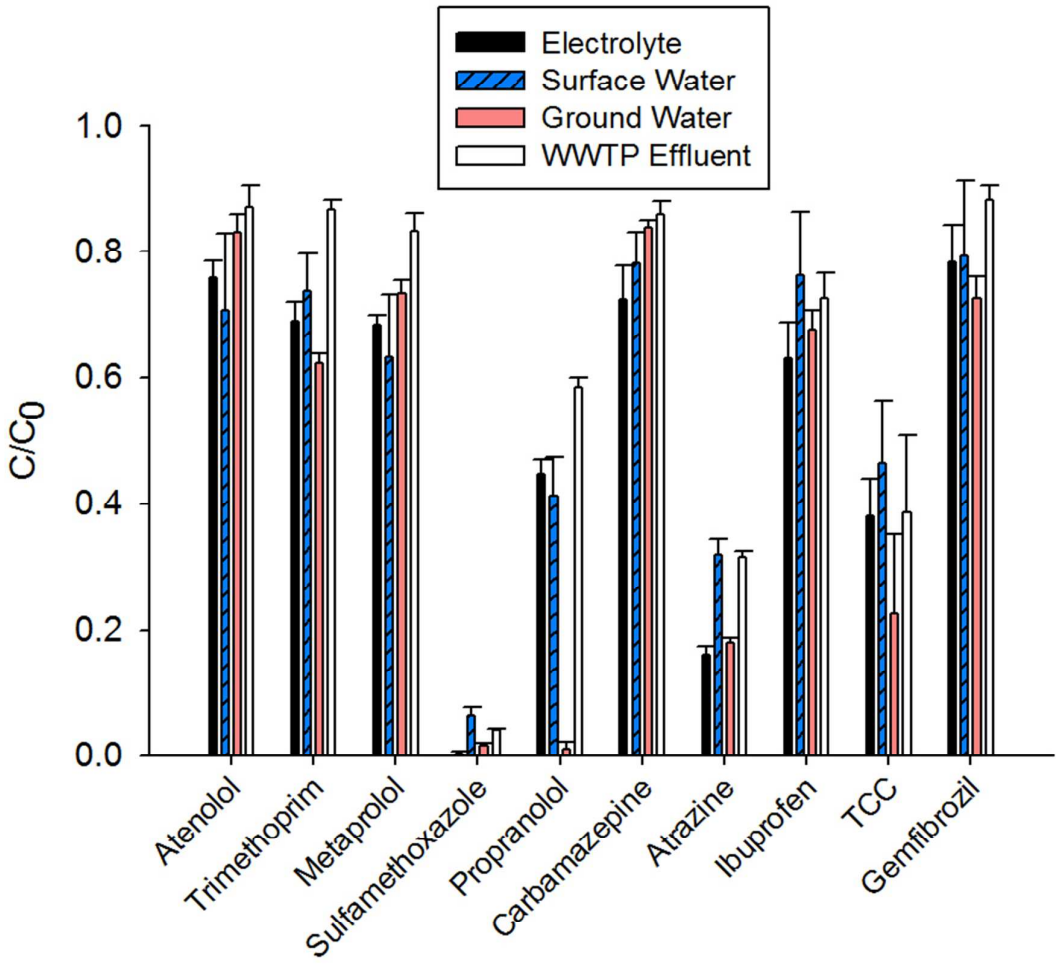

39

40 **Figure S4**: Normalized removal of organic contaminants by UV photolysis (no H_2O_2 present)
41 (WWTP: wastewater treatment plant).

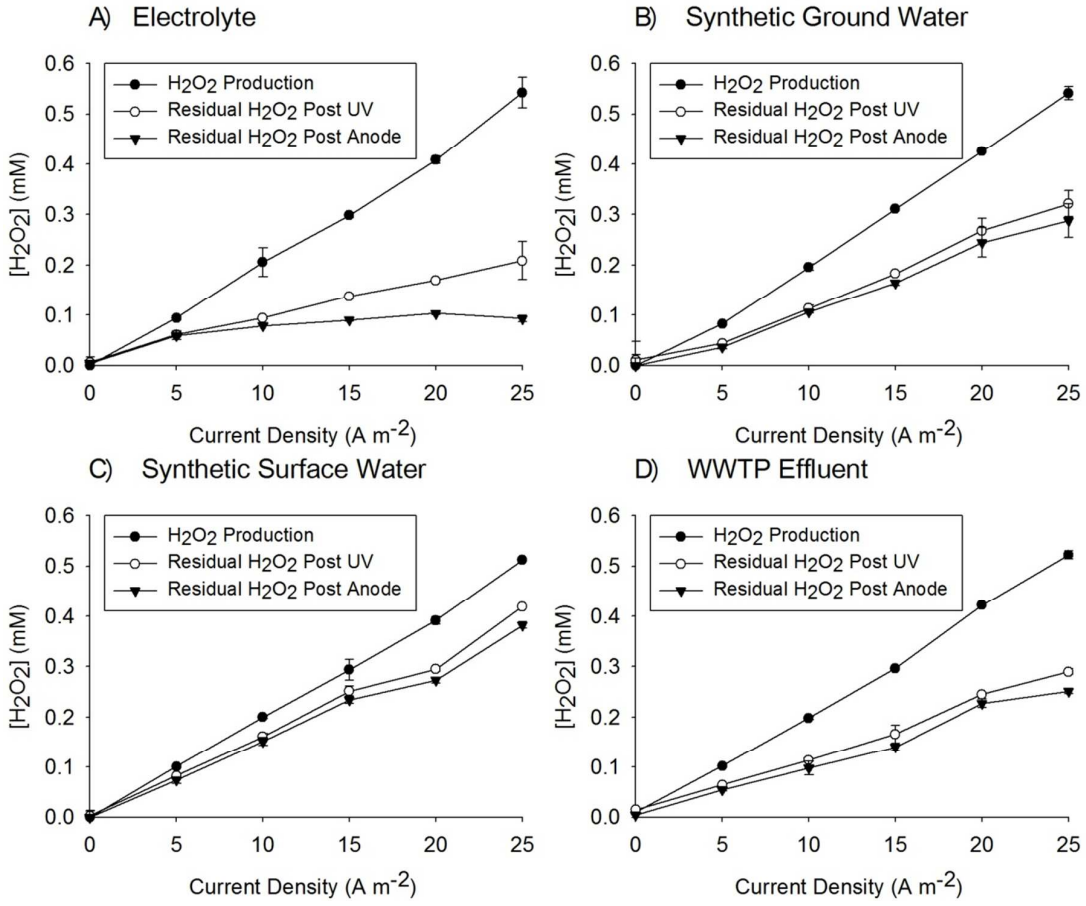

Figure S5: Production of H_2O_2 in the cathode, residual H_2O_2 after the UV cell and residual H_2O_2 after the anode for the four types of source waters at applied current densities from 0 to 25 A m^{-2} (WWTP: wastewater treatment plant).

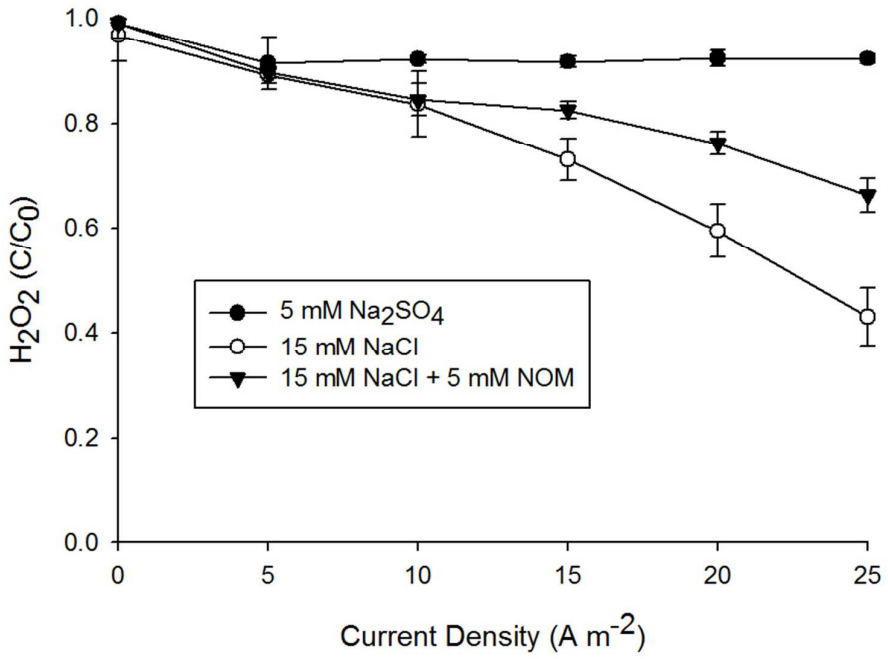

Figure S6: Normalized H_2O_2 removal in the anode as a function of current density in the presence and absence of chloride or natural organic matter (HRT = 1.5 min, $[H_2O_2]_0$ = 10 mg L^{-1} (0.294mM)) (WWTP: wastewater treatment plant).

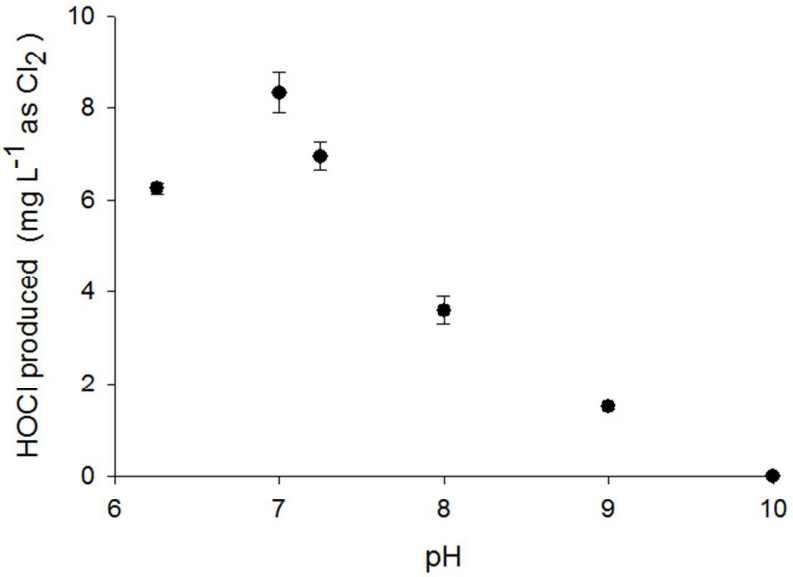

Figure S7: HOCl produced as a function of anodic pH at an applied current density of 25 A m^{-2} ($[Cl^-]_0$ = 10 mM). pH was buffered using 20 mM carbonate buffer (6) and borate buffer (7-10) (WWTP: wastewater treatment plant).

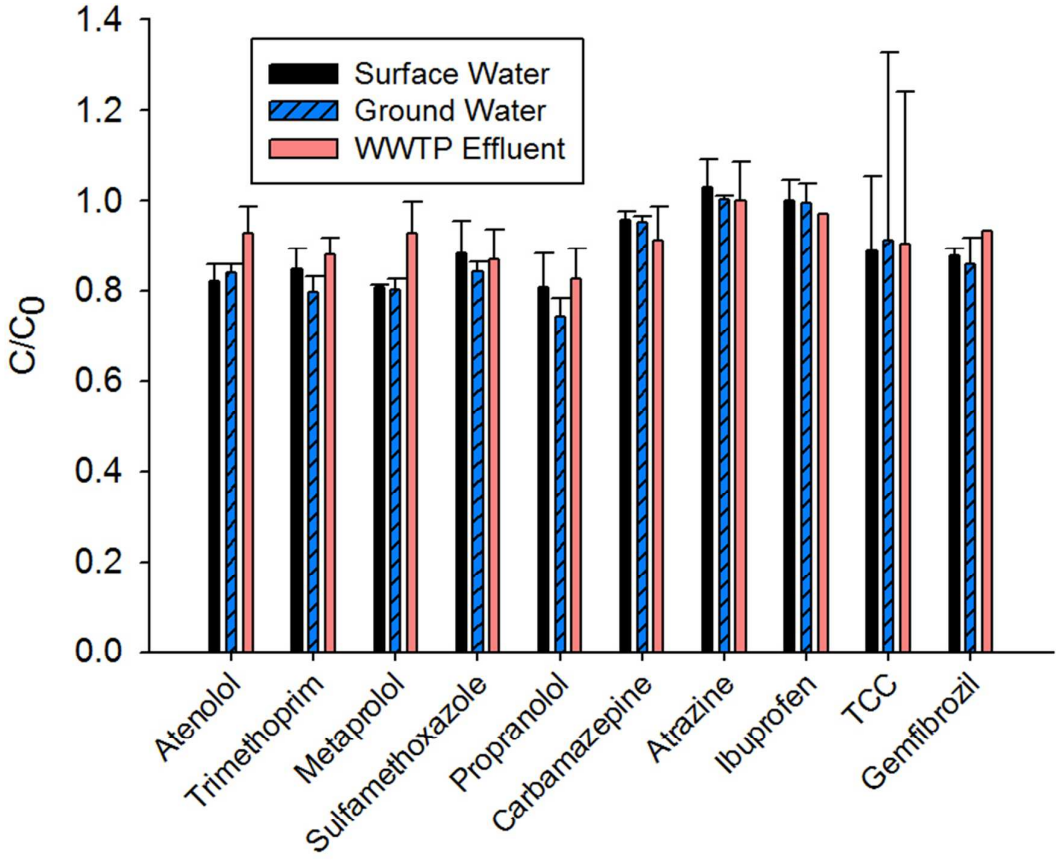

Figure S8: Direct oxidation of trace organic contaminants at 25 A m^{-2} for the 3 representative source waters (HRT = 1.5 min, $[H_2O_2]_0$ = 10 mg L^{-1} (0.294mM)). In the presence of H_2O_2 all $HOCl/OCl^-$ is scavenged and removal of the trace organic contaminants is due to direct anodic oxidation (WWTP: wastewater treatment plant).

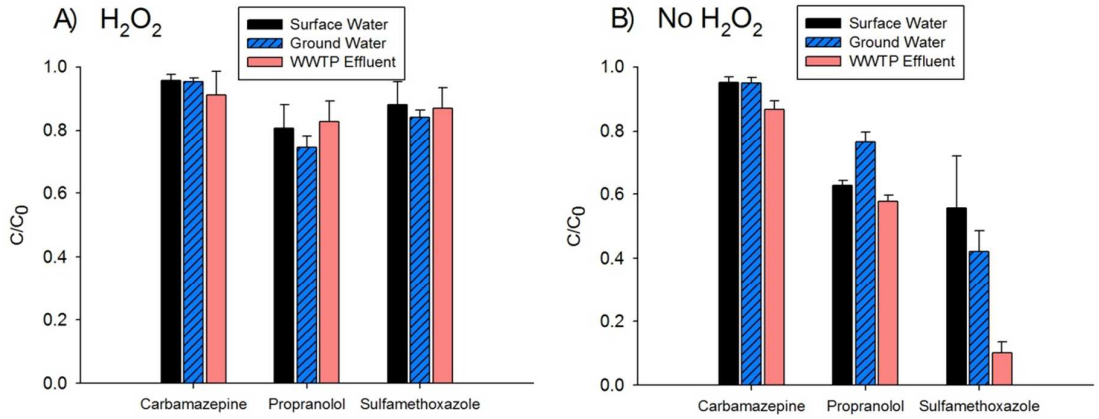

Figure S9: Anodic removal of carbamazepine, propranolol, and sulfamethoxazole in (a) the presence of H_2O_2 (10 mg L^{-1}, chlorine scavenged) and in (b) the absence of H_2O_2 (no chlorine scavenged) at 25 A m^{-2} (HRT = 1.5 min). In the presence of H_2O_2, removal of the trace organic contaminants was due to direct anodic oxidation. In the absence of H_2O_2, removal was due to a combination of direct oxidation and reaction with chlorine. The three compounds were selected because they exhibit varying reactivities with chlorine ($k_{HOCl,carbamazepine}$< $k_{HOCl,propranolol}$< $k_{HOCl,sulfamethoxazole}$; see Table S3) (WWTP: wastewater treatment plant).

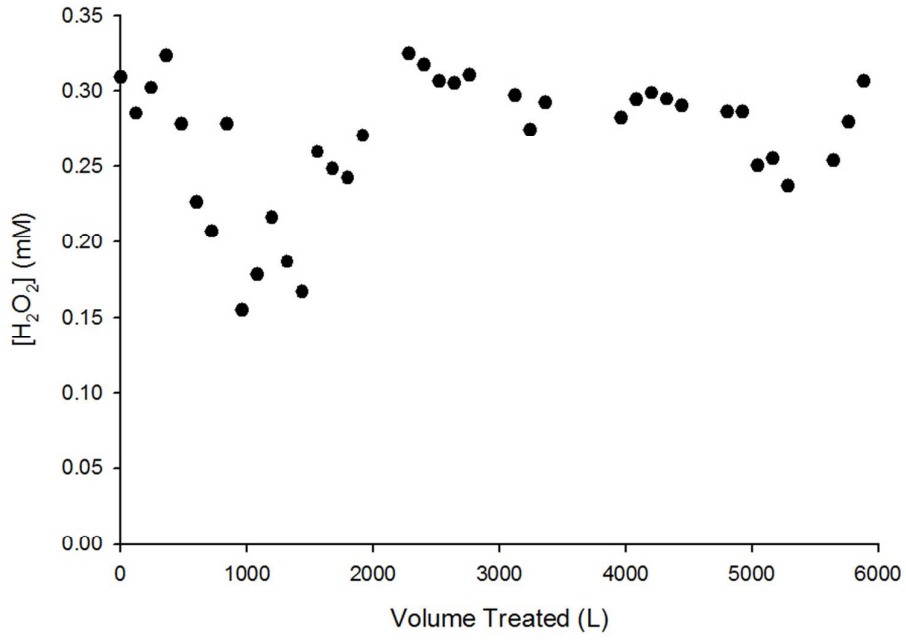

Figure S10: Measured long term cathode performance at 15 A m^{-2} (Catholyte/Anolyte = Tap water + 5mM Na_2SO_4, alkalinity = 0.34 mM, $[Ca^{2+}]$ = 0.2 mM, Q = 120 L d^{-1}). Predicted H_2O_2 production was 0.29 mM (WWTP: wastewater treatment plant).

Determination of the photon fluence rate, W_{254}.

Photon fluence rates at 254 nm were determined using 10 μM atrazine as an actinometer at pH 8[1]. The following constants were employed: ε_{254}=3860 M^{-1} cm^{-1}, ϕ_{254}= 0.046 mol Ei^{-1}. The fluence was calculated from the near surface specific rate of light absorbance for an organic pollutant at a single wavelength:

$$\frac{-d[C]}{dt} = \frac{E^{\circ}_{254}\varepsilon_{254}\varphi_{254}[1-10^{-\alpha z}]}{\alpha z}[C]$$

where E°_{254} is the incident photon fluence rate (Ei m^{-2} s^{-1}) at 254 nm, ε_{254} is the decadic molar extinction coefficient at 254 nm (M^{-1} cm^{-1}), ϕ_{254} is the quantum yield at 254 nm (mol Ei^{-1}), α is the solution absorbance (cm^{-1}), and z is the light path length (cm). Because the experiments were performed in Milli-Q water, we can assume very little light absorbance (i.e., α*z <0.02) and the following approximation can be made:

$$1-10^{-\alpha z} \cong 2.3\alpha z$$

Therefore, the expression for the near surface specific rate of light absorbance simplifies to

$$\frac{-d[C]}{dt} = 2.303E^{\circ}_{254}\varepsilon_{254}\varphi_{254}[C]$$

$$\ln\left(\frac{C}{C_0}\right) = 2.303E^{\circ}_{254}\varepsilon_{254}\varphi_{254}t$$

By plotting the natural logarithm of the contaminant removal with time we can obtain an estimate of the incident photon fluence, E°_{254}:

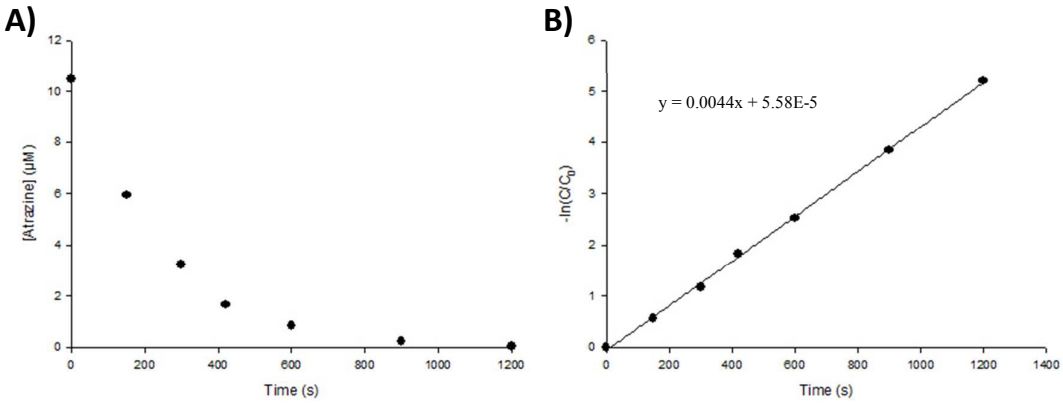

Figure S11: (a) UV photolysis of atrazine versus time and the (b) natural logarithm of

normalized atrazine concentration versus time. The solution contained 10 µM atrazine at pH 8.

$$E^{\circ}_{254} = \frac{k}{2.303\varepsilon_{254}\varphi_{254}}$$

$$E^{\circ}_{254} = 106.8\ \mu Ei\ m^2\ s^{-1}$$

Calculations for the half life of H_2O_2 and NOM with HOCl

In accordance with Zhai et al. (2014), the reaction between HOCl with NOM depends on the number of reactive sites on the NOM, with certain moieties having greater electron donating capacity and therefore higher rates of reaction with HOCl (e.g., phenolic groups). Fast reaction sites are defined as NOM_{fast}, slow reaction sites are defined as NOM_{slow}, and sites that do not produce halogenated byproducts are defined as NOM_{dec}. Using data for SWHA, fast sites comprise about 3% of the aromatic carbon, slow sites comprise 35%, and dec sites comprise 62% [2]. Assuming a $[H_2O_2] = 0.5 \times 10^{-4}$ M (H_2O_2 produced at 25 A m^{-2}) and [NOM] = 5 mg C L^{-1} (0.42 mM), we can calculate the half life of H_2O_2 given the following rate constants: $k_{H2O2,HOCl} = 10^3\ M^{-1}\ s^{-1}$, $k_{HOCl,NOMfast} = 10^3\ M^{-1}\ s^{-1}$, $k_{HOCl,NOMslow} = 1$, $k_{HOCl,NOMdec} = 5\ M^{-1}\ s^{-1}$

$$t_{\frac{1}{2},H2O2} = \frac{\ln(2)}{k_{HOCl,H2O2}[H_2O_2]} = \frac{\ln(2)}{(10^{-3}\ M)(0.5\ x\ 10^{-4}\ M^{-1}\ s^{-1})} = 1.39\ s$$

$$t_{\frac{1}{2},H2O2} = \frac{\ln(2)}{k_{HOCL,NOMfast}[NOM_{fast}] + k_{HOCL,NOMslow}[NOM_{slow}] + k_{HOCL,NOMdec}[NOM_{dec}]}$$

$$= \frac{\ln(2)}{[(0.03)(10^3\ M^{-1}\ s^{-1}) + (0.35)(1\ M^{-1}\ s^{-1}) + (0.62)(5\ M^{-1}\ s^{-1})](4.2 * 10^{-4}\ M)} = 49.3\ s$$

Branching ratio of HOCl with Trace Organics and H_2O_2

Reaction rate constants of HOCl with the trace organic compounds used in this study ranged from 1.7×10^{-2} M^{-1} s^{-1}(atenolol) to 6.17×10^{2} M^{-1} s^{-1}(sulfamethoxazole) (Table S3). Assuming a concentration of trace organics equal to 10^{-6} M (10 compounds at 10 µg L^{-1}, average MW =

250 g mol^{-1}). Using the higher bound on the rate constant with chlorine, the branching ratio of HOCl with trace organics in the presence of H_2O_2 is:

$$\frac{k_{HOCl,organic}[Organic]}{k_{HOCl,H2O2}[H_2O_2]} = \frac{(6.17 \times 10^2\ M^{-1}\ s^{-1})(10^{-6} M)}{(10^{-3}\ M)(10^{-3}\ M^{-1}\ s^{-1})} = 0.0007$$

Therefore, virtually all the HOCl reacts with H_2O_2.

Determination of bimolecular rate constant for HO$^\bullet$ and NOM

In accordance with Appiani et al. (2014), Suwannee River Humic Acids (average molecular weight of 300 g mol^{-1} , %C = 52.55) have a bimolecular rate constant with HO$^\bullet$ of 5.7×10^8 (M_C^{-1} s^{-1}) or 5.6×10^9 (M^{-1} s^{-1})^3. This equates to a bimolecular rate constant on a per carbon basis of 9.8×10^3 (L mgC^{-1} s^{-1}).

Calculation for the fraction of HO$^\bullet$ going to contaminants

$$\text{fraction HO}^\bullet \text{ to contaminants} = \frac{\sum k_{HO^\bullet,cont}[Cont]}{\sum k_{HO^\bullet,s}[S]}$$

A sample calculation for the fraction of the HO$^\bullet$ to trace organic contaminants in the groundwater for pH 8 in the presence of 3 mg L^{-1} (0.09 mM) has been provided using the bimolecular rate constants in Table 1 and Table S3. At pH 8, of the 3.9 mEq L^{-1} of the TIC in the ground water, 3.8 mM is at HCO_3^- while 0.02 mM is as CO_3^{2-}.

$$\frac{\sum k_{HO^\bullet,cont}[Cont]}{\sum k_{HO^\bullet,cont}[Cont] + k_{HO^\bullet,H2O2}[H_2O_2] + k_{HO^\bullet,DOC}[DOC] + k_{HO^\bullet,HCO3}[HCO_3^-] + k_{HO^\bullet,CO32-}[CO_3^{2-}]}$$

$$\frac{(2.99E3\ s^{-1})}{(2.99E3\ s^{-1}) + (2.7E7\ M^{-1}\ s^{-1})(9 * 10^{-5}\ M) + (9.8E3\ L\ mgC^{-1}\ s^{-1})(0.1\ mgC\ L^{-1}) + (8.5E6\ M^{-1}\ s^{-1})(3.8 * 10^{-3}\ M) + (3.9E8\ M^{-1}\ s^{-1})(0.02 * 10^{-5}\ M)}$$

= 6.5% of available HO$^\bullet$

Calculation for the reduction in direct photolysis from H_2O_2 light screening

The pseudo-first order rate constant for direct photolysis of compounds in the absence of H_2O_2, k'_d, is given by:

$$k'_d = \frac{E^\circ_{254}\varepsilon_{254}\varphi_{254}[1-10^{-\alpha z}]}{\alpha z}$$

where E°_{254} is the incident photon fluence rate (Ei m^{-2} s^{-1}) at 254 nm, ε_{254} is the decadic molar extinction coefficient of the organic compound at 254 nm (M^{-1} cm^{-1}), ϕ_{254} is the quantum yield at 254 nm (mol Ei^{-1}), α is the solution absorbance (cm^{-1}), and z is the light path length (cm). In the presence of H_2O_2,the direct photolysis rate decreases due to additional absorbance of incident light by H_2O_2. The pseudo-first order rate constant for direct photolysis of compounds in the presence of H_2O_2, $k'_{d,H2O2}$, is given by:

$$k'_{d,H2O2} = \frac{E^\circ_{254}\varepsilon_{254}\varphi_{254}[1-10^{-(\alpha+\varepsilon_{H2O2}[H_2O_2])z}]}{(\alpha+\varepsilon_{H2O2}[H_2O_2])z}$$

where ε_{H2O2} is the decadic molar extinction coefficient of the H_2O_2 at 254 nm (M^{-1} cm^{-1}). Comparing the two rates, we get:

$$\frac{k'_{d,H2O2}-k'_d}{k'_d} = \frac{\left(\frac{[1-10^{-(\alpha+\varepsilon_{H2O2}[H_2O_2])z}]\alpha}{(\alpha+\varepsilon_{H2O2}[H_2O_2])}\right)-[1-10^{-\alpha z}]}{[1-10^{-\alpha z}]}$$

For WWTP effluent at 25 A m^{-2}: α = 0.137 cm^{-1}, ε_{H2O2}= 18.6 $M^{-1}cm^{-1}$, $[H_2O_2]$ = 0.54 mM , z = 0.043 m. As a result, the direct photolysis rate in the presence of H_2O_2 decreased by 3.8% for the suite of trace organic contaminants:

$$\frac{k'_{d,H2O2}-k'_d}{k'_d} = 0.0378$$

Electrical Energy per Order (E_{EO}) calculation

The following sample calculation is for the E_{EO} of carbamazepine in the nitrified wastewater effluent at a current density of 25 A m^{-2}.

$$E_{EO} = \frac{P}{Q\log\left(\frac{C_0}{C}\right)}$$

where P (kW) is the electrical power for the electrochemical cell and UV lamp, Q ($m^3\ h^{-1}$) is the system flow rate, and C_0 and C (M) are the initial and final contaminant concentrations.

$$Q = \left(\frac{120\ L}{d}\right)\left(\frac{m^3}{1000L}\right)\left(\frac{d}{24h}\right) = 0.005\frac{m^3}{h}$$

The total system power (P_{total},W) is a combination of the UV lamp power and the electrochemical cell power, which can be expressed as a product of the current density (I, A m^{-2}), cell potential (V_{cell}), and the electrode surface area (A, m^2) :

$$P_{total} = I * A * V_{cell} + P_{lamp}$$

$$P_{total} = \left(\frac{25\ A}{m^2}\right)(0.0064\ m^2)(6.67\ V) + 9W = 10.1\ W = 0.01\ kW$$

At 25 A m^{-2}, carbamazepine was transformed from 10.18 ± 0.3 μg L^{-1} (4.3×10^{-8} M) to 0.63 ± 0.03 μg L^{-1} (2.7×10^{-9} M).

$$E_{EO} = \frac{0.01\ kW}{\left(0.005\frac{m^3}{h}\right)\log\left(\frac{4.3\ \times\ 10^{-8}\ M}{2.7\ \times\ 10^{-9}\ M}\right)} = 1.67\ kWh\log^{-1}m^{-3}$$

Energy and energy per volume treated calculations for the electrochemical cell and UV lamp

At a current density of 4.14 A m^{-2}, the highest cell potential was for the poorly conductive groundwater (2.67 V). Assuming the cell runs continuously for a day:

$$\left(\frac{4.14\ A}{m^2}\right)(0.0064\ m^2)(2.67\ V) = 0.071\ W = \frac{0.071\ J}{s}$$

$$\left(\frac{0.071\ J}{s}\right)(86400s)\left(\frac{Wh}{3600J}\right) = 1.7\ Wh$$

The energy per volume of water treated was calculated using the power output of the UV lamp (9W) and the flow rate of the system (120 L d^{-1})

$$(0.009\ kW)\left(\frac{1d}{120L}\right)\left(\frac{24h}{d}\right)\left(\frac{1000L}{m^3}\right) = 1.8\ kWh\ m^{-3}$$

pH dependence of H_2O_2 reaction with HOCl

The primary mechanisms for the reaction of HOCl with H_2O_2 are:

$$HOCl + HO_2^- \xrightarrow{k_1=4.4E7\ M^{-1}\ s^{-1}} Cl^- + O_2 + H_2O$$

$$OCl^- + H_2O_2 \xrightarrow{k_2=3.4E3\ M^{-1}\ s^{-1}} Cl^- + O_2 + H_2O$$

The removal of either $HOCL_{total}$ or $H_2O_{2\ total}$ can be given by

$$\frac{-d[HOCl_{total}]}{dt} = (k_1\alpha_{0,HOCl}\alpha_{1,H202} + k_2\alpha_{1,HOCl}\alpha_{0,H202})[HOCl_{total}][H_2O_{2_{total}}]$$

Where the pH dependent biomolecular rate constant is just:

$$k'_{pH} = (k_1\alpha_{0,HOCl}\alpha_{1,H202} + k_2\alpha_{1,HOCl}\alpha_{0,H202})$$

Given the $pK_{a,HOCl} = 7.6$ and $pK_{a,H2O2} = 11.6$, we can calculate the alpha speciation values.

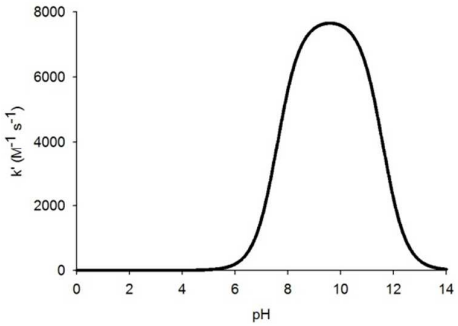

Figure S12: pH-dependent bimolecular rate constant for the reaction between HOCl and H_2O_2.

Table S1. Composition of the waters

Cations (mM)	Electrolyte	Surface Water	Ground Water	WWTP Effluent[b]
Na^+	12.5	1.12	0.0256	13.9
K^+	0	0.234	0.11	0.41
Ca^{2+}	0	2.55	0.81	1.8
Mg^{2+}	0	0.383	0.5	1.68
Anions (mM)				
NO_3^-	0	0.234	0.11	1.63
SO_4^{2-}	0	0.558	0.2	1.68
Cl^-	12.5	1.15	0.6	9.35
PO_4^{3-}	0	0	0.0128	0.069
Ionic Strength[a]	12.5	13.2	6.6	25.6
TIC (mM)	0	2.42	3.89	5.00
DOC (mg/L)	0	1.55	0	4.91

[a]Carbonate contribution to ionic strength calculated using speciation the speciation of TIC at the initial pH of the waters. [b]Nitrified wastewater effluent was obtained from the Discovery Bay municipal wastewater treatment plant (Discovery Bay, CA).

Electrolyte, simulated surface water, and simulated groundwater were prepared in 18 MΩ Milli-Q water. Un-disinfected, nitrified wastewater effluent from the adjacent oxidation ditch treatment plant was obtained from the Discovery Bay municipal wastewater treatment plant (Discovery Bay, CA).

Trace organic compounds were separated by an Agilent 1200 HPLC using a 3.0 mm × 150 mm Phenomenex Synergi Hydro-RP 4 μm column, after a 3.00 mm × 4 mm AQ C18 SecurityGuard guard cartridge. The column was eluted with 0.6 mL min^{-1} methanol and 0.1% acetic acid in water with the following gradient: 0 minutes, 0% methanol; 2 minutes, 0% methanol; 8 minutes, 60% methanol; 11 minutes, 95% methanol; 12 minutes, 95% methanol; 12.1 minutes, 0% methanol; 17 minutes, 0% methanol. Compounds were detected with an Agilent 6460 MS-MS using electrospray ionization (ESI) with a gas temperature of 350°C, a sheath gas temperature of 400°C, a gas flow rate of 11 L/min at 50 psi, and a capillary voltage of 3600 V. Compound-specific parameters are given in Table SI 2.

Table S2. Compound-Specific Mass Spectrometry Parameters[a]

compound	precursor ion (amu)	fragmentor voltage (V)	product ions (amu)	collision energy (V)	cell accelerator (V)	ionization mode
Atenolol	267	130	145 190	24 16	7	positive[b]
Atrazine	216.1	100	173.9 104	30 15	3 3	positive
Carbamazepine	237	120	179 194	35 15	7	positive
Gemfibrozil	249	75	121	5	3	negative[c]
Ibuprofen	205	50	161	0	3	negative
Metoprolol	268	130	159 116	17 14	7	positive
Propranolol	260	98	116 183	13 12	7	positive
Sulfa-methoxazole	254	110	92 156	25 10	7	positive
Trimethoprim	291	140	123 261	20 17	7	positive

[a]All compounds were analyzed using a drying gas temperature of 350° C, a gas flow of 12 L min^{-1}, a nebulizer pressure of 60 psi, a sheath gas temperature of 400 ° C, a sheath gas flow of 12 L min^{-1}, a nozzle voltage of 300 V, and a dwell time of 7 ms. [b]Compounds analyzed by positive ionization used a capillary voltage of 3600 V. [c]Compounds analyzed by negative ionization used a capillary voltage of 4500 V.

200 **Table S3**. Compound Specific Properties

	Property						
Compound	ε_{254} (M^{-1} cm^{-1})[4]	Φ_{254} (mol Ei^{-1})[4]	pK_a	log K_{ow}	$k_{HO\bullet,cont}$ (M^{-1} s^{-1})	$k_{CO_3\bullet^-,cont}$ (M^{-1} s^{-1})	$k_{HOCl,cont}$ (M^{-1} s^{-1})
Atenolol	5.27×10^2	1.1×10^{-2}	9.6	0.2-0.5	7.5×10^9 [5]	5.9×10^7 [6]	1.7×10^{-2} [7]
Trimethoprim	2.64×10^3	1.49×10^{-3}	9.5	1.9-2.3	8.7×10^9 [8]	3.5×10^7 [6, 9]	1.6×10^2 [10]
Metoprolol	1.9×10^2	1.18×10^{-2}	9.1	3.4	8.4×10^9 [6]	-	1.7×10^{-2} [7]
Sulfamethoxazole	6.92×10^3	9.0×10^{-2}	7.4	0.9	5.9×10^9 [6]	4.4×10^8 [6]	6.17×10^2 [10]
Propranolol	1.03×10^3	5.2×10^{-3}	5.6	0.9	1.1×10^{10} [6]	4.6×10^8 [6]	7.5×10^0 [7]
Carbamazepine	5.27×10^2	1.3×10^{-4}	13.9	2.5	9.1×10^9 [6]	2.3×10^6 [6]	< 0.1 [11]
Atrazine	3.86×10^3	4.6×10^{-2}	3.2	2.7	3×10^9 [12]	-	-
Ibuprofen	1.24×10^3	1.12×10^{-2}	4.91	2.5	6.7×10^9 [13]	-	< 0.1 [11]
Gemfibrozil	n.d.	1.23×10^{-2}	4.77	4.8	1.0×10^{10} [14]	-	7.3×10^{-1} [7]

201

202

203

204

205

206

207

208

209

210

Table S4. Normalized Total System Pharmaceutical Transformation for Electrolyte

	Atenolol	Trimethoprim	Metoprolol	Sulfamethoxazole	Propranolol	Carbamazepine	Atrazine	Ibuprofen	TCC	Gemfibrozil
No EC/ NO UV	1.00 ± 0	1.00 ± 0	1.00 ± 0	1.00 ± 0	1.00 ± 0	1.00 ±0	1.00 ± 0	1.00 ± 0	1.00 ± 0	1.00 ± 0
0 + UV	0.758 ± 0.027	0.689 ± 0.030	0.684 ± 0.015	0.000	0.447 ± 0.023	0.724 ± 0.053	0.162 ± 0.013	0.630 ± 0.057	0.383 ± 0.060	0.782 ± 0.060
5+ UV	0.00	0.000	0.014 ± 0.010	0.000	0.006 ± 0.002	0.000	0.06 ± 0.008	0.033 ± 0.007	0.328 ± 0.085	0.018 ± 0.010
10 + UV	0.00	0.000	0.004 ± 0.006	0.000	0.003 ± 0.002	0.000	0.0531 ± 0.009	0.017 ± 0.017	0.678 ± 0.359	0.000
15+ UV	0.00	0.000	0.00 ± 0.001	0.000	0.003 ± 0.002	0.000	0.052 ± 0.007	0.022 ± 0.014	0.439 ± 0.190	0.000
20+ UV	0.00	0.000	0.000	0.000	0.001 ± 0.001	0.000	0.058 ± 0.002	0.018 ± 0.011	0.449 ± 0.288	0.000
25+UV	0.00	0.000	0.001 ± 0.002	0.000	0.000	0.000	0.068 ± 0.007	0.027 ± 0.005	0.319 ± 0.143	0.000

Table S5. Normalized Total System Pharmaceutical Transformation for Synthetic Groundwater

	Atenolol	Trimethoprim	Metoprolol	Sulfamethoxazole	Propranolol	Carbamazepine	Atrazine	Ibuprofen	TCC	Gemfibrozil
No EC/ NO UV	1.00 ± 0	1.00 ± 0	1.00 ± 0	1.00 ± 0	1.00 ± 0	1.00 ±0	1.00 ± 0	1.00 ± 0	1.00 ± 0	1.00 ± 0
0 + UV	0.829 ± 0.030	0.622 ± 0.016	0.734 ± 0.020	0.016 ± 0	0.011 ± 0.012	0.838 ± 0.012	0.180 ± 0.001	0.676 ± 0.03	0.226 ± 0.127	0.725 ± 0.035
5+ UV	0.153 ± 0.013	0.0131 ± 0.005	0.125 ± 0.006	0	0.0018 ± 0	0.215 ± 0.012	0.104 ± 0.004	0.265 ± 0.015	0.288 ± 0.099	0.212 ± 0.01
10 + UV	0.066 ± 0.01	0.0064 ± 0.007	0.071 ± 0.01	0	0.0035 ± 0	0.118 ± 0.014	0.098 ± 0.014	0.151 ± 0.032	0.394 ± 0.218	0.155 ± 0.02
15+ UV	0.041 ± 0	0	0.032 ± 0.028	0	0.0017 ± 0	0.07 ± 0	0.090 ± 0.002	0.133 ± 0.009	0.3 ± 0.064	0.118 ± 0
20+ UV	0.0175 ± 0.003	0	0.032 ± 0.001	0	0.0055 ± 0	0.047 ± 0.04	0.082 ± 0.004	0.133 + 0.01	0.241 ± 0.08	0.093 ± 0.005
25+UV	0.009 ± 0.003	0	0.025 ± 0.002	0	0.002 ± 0	0.013 ± 0.01	0.077 ± 0.002	0.089 ± 0.03	0.333 ± 0.118	0.081 ±0.002

Table S6. Normalized Total System Pharmaceutical Transformation for Wastewater Effluent

	Atenolol	Trimethoprim	Metoprolol	Sulfamethoxazole	Propranolol	Carbamazepine	Atrazine	Ibuprofen	TCC	Gemfibrozil
No EC/ NO UV	1.00 ± 0	1.00 ± 0	1.00 ± 0	1.00 ± 0	1.00 ± 0	1.00 ±0	1.00 ± 0	1.00 ± 0	1.00 ± 0	1.00 ± 0
0 + UV	0.871 ± 0.033	0.866 ± 0.015	0.831 ± 0.029	0.042 ± 0.002	0.585 ± 0.013	0.858 ± 0.022	0.316 ± 0.010	0.725 ± 0.040	0.386 ± 0.123	0.882 ± 0.023
5+ UV	0.577 ± 0.083	0.553 ± 0.083	0.523 ± 0.071	0.022 ± 0.006	0.195 ± 0.028	0.485 ± 0.049	0.264 ± 0.01	0.501 ± 0.071	0.285 ± 0.067	0.559 ± 0.068
10 + UV	0.443 ± 0.018	0.429 ± 0.025	0.382 ± 0.029	0.010 ± 0.01	0.090 ± 0.011	0.331 ± 0.025	0.250 ± 0.024	0.429 ± 0.093	0.241 ± 0.052	0.441 ± 0.073
15+ UV	0.400 ± 0.051	0.390 ± 0.042	0.331 ± 0.047	0.005 ± 0.004	0.055 ± 0.007	0.271 ± 0.029	0.239 ± 0.015	0.374 ± 0.071	0.463 ± 0.131	0.366 ± 0.041
20+ UV	0.378 ± 0.060	0.359 ± 0.061	0.313 ± 0.055	0.013 ± 0.002	0.051 ± 0.008	0.260 ± 0.057	0.289 ± 0.021	0.228 ± 0.144	0.349 ± 0.246	0.209 ± 0.189
25+UV	0.324 ± 0.039	0.313 ± 0.036	0.265 ± 0.025	0.009 ± 0	0.032 ± 0.006	0.215 ± 0.019	0.278 ± 0.011	0.234 ± 0.133	0.515 ± 0.221	0.179 ± 0.144

Table S7. Normalized Total System Pharmaceutical Transformation for Surface Water

	Atenolol	Trimethoprim	Metoprolol	Sulfamethoxazole	Propranolol	Carbamazepine	Atrazine	Ibuprofen	TCC	Gemfibrozil
No EC/ NO UV	1.00 ± 0	1.00 ± 0	1.00 ± 0	1.00 ± 0	1.00 ± 0	1.00 ±0	1.00 ± 0	1.00 ± 0	1.00 ± 0	1.00 ± 0
0 + UV	0.706 ± 0.12	0.737 ± 0.06	0.632 ± 0.10	0.063 ± 0.014	0.414 ± 0.06	0.781 ± 0.050	0.320 ± 0.024	0.762 ± 0.1	0.463± 0.123	0.792 ± 0.13
5+ UV	0.181 ± 0.033	0.156 ± 0.006	0.155 ± 0.029	0.024 ± 0.002	0.065 ± 0.014	0.160 ± 0.012	0.193 ± 0.016	0.172 ± 0.0166	0.205 ± 0.095	0.043 ± 0.006
10 + UV	0.081 ± 0.016	0.086 ± 0.008	0.065 ± 0.017	0.015 ± 0.004	0.036 ± 0.087	0.080 ± 0.010	0.148 ± 0.012	0.134 ± 0.027	0.406 ± 0.194	0.117 ± 0.033
15+ UV	0.074 ± 0.004	0.072 ± 0.003	0.068 ± 0.003	0.012 ± 0.001	0.048 ± 0.007	0.074 ± 0.005	0.144 ± 0.005	0.084 ± 0.030	0.465 ± 0.35	0.071 ± 0.022
20+ UV	0.076 ± 0.024	0.087 ± 0.021	0.063 ± 0.02	0.020 ± 0.007	0.043 ± 0.012	0.065 ± 0.000	0.190 ± 0.0276	0.193 ± 0.073	0.368 ± 0.154	0.157 ± 0.064
25+UV	0.068 ± 0.013	0.070 ± 0.017	0.058 ± 0.017	0.010 ± 0.005	0.040 ± 0.012	0.067 ± 0.01	0.152 ± 0.020	0.166 ± 0.034	0.251 ± 0.013	0.113 ± 0.024

REFERENCES

1. Canonica, S.; Meunier, L.; Von Gunten, U., Phototransformation of selected pharmaceuticals during UV treatment of drinking water. *Water Research* **2008,** *42*, (1-2), 121-128.
2. Zhai, H.; Zhang, X.; Zhu, X.; Liu, J.; Ji, M., Formation of Brominated Disinfection Byproducts during Chloramination of Drinking Water: New Polar Species and Overall Kinetics. *Environmental Science & Technology* **2014,** *48*, (5), 2579-2588.
3. Appiani, E.; Page, S. E.; McNeill, K., On the Use of Hydroxyl Radical Kinetics to Assess the Number-Average Molecular Weight of Dissolved Organic Matter. *Environmental Science & Technology* **2014,** *48*, (20), 11794-11802.
4. Jasper, J. T.; Jones, Z. L.; Sharp, J. O.; Sedlak, D. L., Biotransformation of trace organic contaminants in open-water unit process treatment wetlands. *Environmental Science & Technology* **2014,** *48*, (9), 5136-5144.
5. Salgado, R.; Pereira, V. J.; Carvalho, G.; Soeiro, R.; Gaffney, V.; Almeida, C.; Cardoso, V. V.; Ferreira, E.; Benoliel, M. J.; Ternes, T. A.; Oehmen, A.; Reis, M. A. M.; Noronha, J. P., Photodegradation kinetics and transformation products of ketoprofen, diclofenac and atenolol in pure water and treated wastewater. *Journal of Hazardous Materials* **2013,** *244*, 516-527.
6. Jasper, J. T.; Sedlak, D. L., Phototransformation of Wastewater-Derived Trace Organic Contaminants in Open-Water Unit Process Treatment Wetlands. *Environmental Science & Technology* **2013,** *47*, (19), 10781-10790.
7. Pinkston, K. E.; Sedlak, D. L., Transformation of aromatic ether-and amine-containing pharmaceuticals during chlorine disinfection. *Environmental Science & Technology* **2004,** *38*, (14), 4019-4025.
8. Baeza, C.; Knappe, D. R. U., Transformation kinetics of biochemically active compounds in low-pressure UV Photolysis and UV/H_2O_2 advanced oxidation processes. *Water Research* **2011,** *45*, (15), 4531-4543.
9. Zhang, R.; Sun, P.; Boyer, T. H.; Zhao, L.; Huang, C.-H., Degradation of Pharmaceuticals and Metabolite in Synthetic Human Urine by UV, UV/H_2O_2, and UV/PDS. *Environmental Science & Technology* **2015,** *49*, (5), 3056-3066.
10. Deborde, M.; von Gunten, U., Reactions of chlorine with inorganic and organic compounds during water treatment - Kinetics and mechanisms: A critical review. *Water Research* **2008,** *42*, (1-2), 13-51.
11. Lee, Y.; von Gunten, U., Oxidative transformation of micropollutants during municipal wastewater treatment: Comparison of kinetic aspects of selective (chlorine, chlorine dioxide, ferrate(VI), and ozone) and non-selective oxidants (hydroxyl radical). *Water Research* **2010,** *44*, (2), 555-566.
12. Acero, J. L.; Stemmler, K.; Von Gunten, U., Degradation kinetics of atrazine and its degradation products with ozone and OH radicals: A predictive tool for drinking water treatment. *Environmental Science & Technology* **2000,** *34*, (4), 591-597.
13. Shu, Z. Q.; Bolton, J. R.; Belosevic, M.; El Din, M. G., Photodegradation of emerging micropollutants using the medium-pressure UV/H_2O_2 Advanced Oxidation Process. *Water Research* **2013,** *47*, (8), 2881-2889.
14. Razavi, B.; Song, W. H.; Cooper, W. J.; Greaves, J.; Jeong, J., Free-Radical-Induced Oxidative and Reductive Degradation of Fibrate Pharmaceuticals: Kinetic Studies and Degradation Mechanisms. *Journal of Physical Chemistry A* **2009,** *113*, (7), 1287-1294.